X-325-72-452

NASA TM X- 66137

A MEASUREMENT OF THE RELATIVE CROSS SECTIONS FOR SIMULTANEOUS IONIZATION AND EXCITATION OF THE DEGENERATE He^+ n = 4 LEVELS

J. F. SUTTON
R. B. KAY

OCTOBER 1972

GSFC — GODDARD SPACE FLIGHT CENTER —
GREENBELT, MARYLAND

X-325-72-452

A MEASUREMENT OF THE RELATIVE CROSS SECTIONS FOR SIMULTANEOUS IONIZATION AND EXCITATION OF THE DEGENERATE He^+ n = 4 LEVELS

J. F. Sutton

R. B. Kay

October 1972

GODDARD SPACE FLIGHT CENTER

Greenbelt, Maryland

A MEASUREMENT OF THE RELATIVE CROSS SECTIONS FOR SIMULTANEOUS IONIZATION AND EXCITATION OF THE DEGENERATE He^+ n = 4 LEVELS

J. F. Sutton

R. B. Kay

ABSTRACT

The relative cross sections for simultaneous ionization and excitation of helium by 200 eV electrons into the 4S, 4P, 4D and 4F levels have been measured via a fast delayed coincidence technique. Results are in poor agreement with Born approximation calculations for simultaneous ionization and excitation of helium, the 4P component being larger than expected.

CONTENTS

ILLUSTRATIONS

ILLUSTRATIONS (Continued)

TABLES

A MEASUREMENT OF THE RELATIVE CROSS SECTIONS FOR SIMULTANEOUS IONIZATION AND EXCITATION OF THE DEGENERATE He^+ n = 4 LEVELS

Studies of simultaneous ionization and excitation of atoms by electron impact began receiving attention in the last several years, particularly for the noble gases helium and argon.[1, 2, 3, 4, 5, 6, 7] We have chosen to study the problem in helium, as the theoretical calculations are considerably more reliable and tractable in its case. An experimental study which could identify the final atomic levels in angular momentum quantum number at the n = 4 level was undertaken, as the results would provide a much stronger test of the ability of 1st order Born amplitudes to adequately describe such a complicated excitation. The experimental problem, however, is difficult, as the final He^+ levels are nearly energy degenerate with respect to angular momentum quantum number and must either be studied by interferometry or time resolved spectroscopy. We chose the latter technique, as the light collecting efficiency of the associated optics is considerably greater, and the cross sections to be studied are quite small.

For the most part previous experimental studies of the simultaneous ionization and excitation of He have been limited to measuring the line strength from the upper level complex to a lower level. Hughes and Weaver studied the ionization-excitation of the n = 4 complex and found a n = 4 → n = 3 line cross section of Q (4686 Å) = 10.2×10^{-21} cm^2 [see Fig. 1]. St. John and

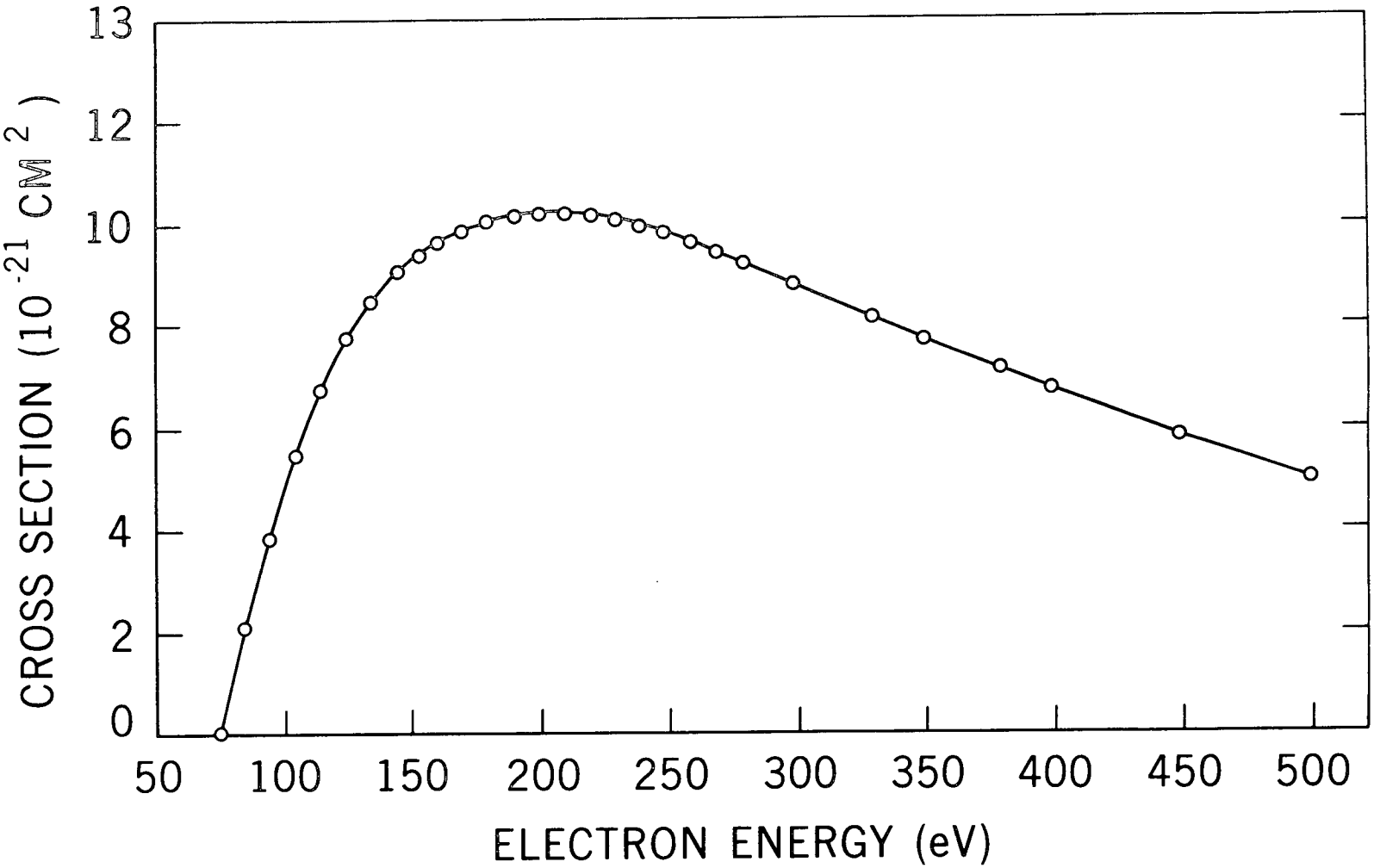

Figure 1. Total cross section, QHe^+ (4 → 3) vs. impact electon energy (Hughes and Weaver).

Lin measured Q (4686 Å) = 3.7×10^{-21} cm^2, and then revised their result to Q (4686 Å) = 9.8×10^{-21} cm^2 at ~200 eV.[2] The revised measurement of St. John and Lin and that of Hughes and Weaver should show the good agreement they do, as they are both referred to the same "standard" line. More recently, M. R. Moustafa Moussa and F. J. DeHeer have measured the Q (4686 Å) $\approx 4.85 \times 10^{-21}$ cm^2, at ~200 eV, and further, they find an $(energy)^{-1}$ dependence in the cross section for energies up to 3 keV.[4] This energy dependence is normally associated with quadrupole (and higher order) terms in the 1st Born-Bethe expansion. Anderson and Hughes[8] have recently reported a time resolved study of the 4686 Å radiation. While finding some information about the long-lived components present, the time resolution of their apparatus was not sufficient to separate out the important fast components associated with the P, D, and F excitations in the complex.[9]

Dalgarno and McDowell[10], using the Born approximation, calculated cross sections for the process

$$e + He \rightarrow e + He^+ (nl) + e \text{ for } nl = 4P, \text{ and } 4D.$$

Due to a large degree of arbitrariness in the choice of the initial and final wave functions, errors of the order of a factor-of-five were predicted.

Lee and Lin[11] extended the Born Approximation calculations of Dalgarno and McDowell to include the 4S state. By using the 4P and 4D calculations of Dalgarno and McDowell as a guide for choosing a value of effective nuclear charge, they also calculated cross sections for the 4F state. The results of their calculations suggested that about 90% of the total 4 → 3 emission is due to

the 4S → 3P transition. This is because the 4S state can cascade only to 3P and 2P, whereas the majority of the atoms in 4P cascade to 1S leaving only a small fraction of the 4P population for the 4P → 3S and 4P → 3D transitions. (See Fig. 2.) Using these results, the total absolute cross section was calculated to be $Q\,(He^+)_{max}\ (4 \rightarrow 3) = 3.7 \times 10^{-21}\ cm^2$, which compares better to the work of DeHeer et. al., although it must be noted that all the maximum experimental line cross sections are higher than theoretically predicted. This is curious as the Born approximation usually overestimates the peak cross sections. The experimental and theoretical results are summarized in Table I.

Knowledge of the relative cross sections to the n = 4 He^+ complex has an important applied aspect. The measurement of the 4686 Å 4 → 3 radiation by standard lamp would allow an accurate prediction of the 4 → 2 1215 Å radiation, yielding a very accessible standard line for Lyman alpha measurements.

Experimental Method

The delayed coincidence technique[12] was used to study the He^+ (4 → 3) transitions. A fast pulse generator with rise- and decay-times of 0.3 nsec was used to drive the cathode of a modified 7587 tetrode Nuvistor electron gun. The resulting electron beam simultaneously ionized and excited a small percentage of the helium atoms resulting in the radiation of photons from the hydrogen-like He^+ ions. These photons were detected by a fast photomultiplier tube (PMT). A pair of narrow band dielectric filters were employed for wavelength selection.

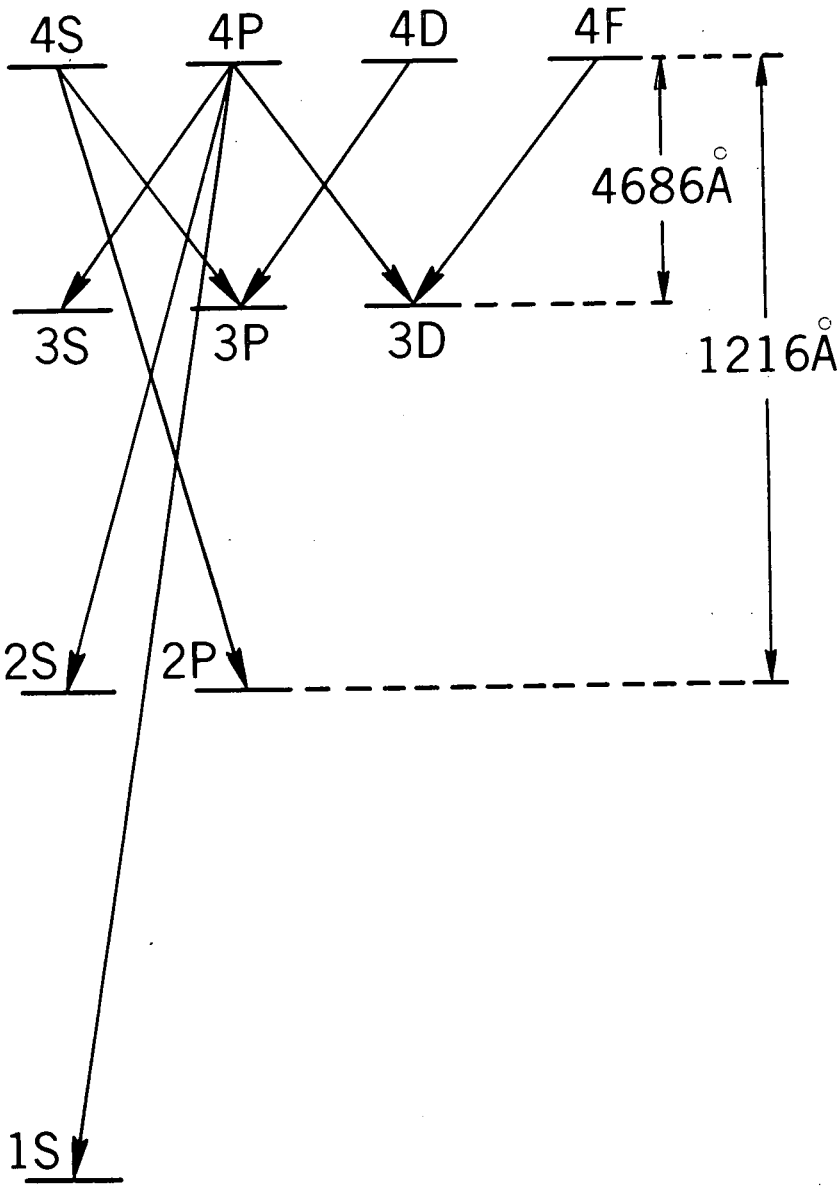

Figure 2. Partial Grotrian diagram for He^+, showing the possible modes of decay in the n = 4 → n = 3 complex.

Table I

Comparison of Theoretical and Experimental Cross Sections

for Simultaneous Ionization and Excitation in Helium.[11]

	Incident Electron Energy (eV)				
	200	270	340	405	450
$Q(He^+, 4S)$	8.1	8.2	7.6	6.9	6.6
$Q(He^+, 4P)$	2.9	3.1	2.9	2.8	2.7
$Q(He^+, 4D)$	0.68	0.69	0.66	0.62	0.57
$Q(He^+, 4 \rightarrow 3)$, theory	3.7	3.8	3.5	3.2	3.0
$Q(He^+, 4 \rightarrow 3)$, experiment	9.8	9.1	7.9	7.0	6.5
$Q(He^+, 5S)$	3.8	3.8	3.5	3.2	3.0
$Q(He^+, 5P)$	1.4	1.4	1.4	1.3	1.3
$Q(He^+, 5D)$	0.36	0.36	0.34	0.32	0.30
$Q(He^+, 5 \rightarrow 3)$, theory	1.4	1.4	1.3	1.2	1.1
$Q(He^+, 5 \rightarrow 3)$, experiment	2.6	2.8	2.4	--	--
$Q(He^+, 6S)$	2.1	2.1	1.9	1.8	1.7
$Q(He^+, 6P)$	0.78	0.80	0.77	0.74	0.71
$Q(He^+, 6D)$	0.13	0.12	0.10	0.09	0.08
$Q(He^+, 6 \rightarrow 3)$, theory	0.63	0.63	0.59	0.54	0.51
$Q(He^+, 6 \rightarrow 3)$, experiment	1.9	1.8	1.7	--	--
$Q(He^+, 7S)$	1.3	1.3	1.2	1.1	1.0
$Q(He^+, 7P)$	0.48	0.49	0.48	0.45	0.44
$Q(He^+, 7D)$	0.08	0.49	0.48	0.45	0.44
$Q(He^+, 7 \rightarrow 3)$, theory	0.08	0.08	0.07	0.06	0.05
$Q(He^+, 7 \rightarrow 3)$, experiment	0.35	0.35	0.31	0.29	0.27

Cross sections (in 10^{-21} cm^2) for ionization excitation of Helium by electron impact.

The PMT pulses were used to start the conversions in a time-to-pulse-height converter (TPH), while the pulse generator signal was used to stop them. This reversed sequence significantly reduced TPH dead time. A constant fraction timing discriminator was used to eliminate "walk" errors due to variations in PMT pulse amplitudes. The TPH output was accumulated in the memory of a multichannel analyzer (MCA) for later digital computer analysis. Figure 3 is a block diagram of the apparatus.

In order to accentuate the fast 0.8 nsec lifetime He^+ (4P) radiation relative to the slow 14 nsec lifetime He^+ (4S) component, a short (1.2 nsec) excitation pulse was used. A high repetition rate of 1 MHz was necessary due to the small cross sections involved. The 7587 Nuvistor electron gun was modified by welding short ground leads to the control grid supports. The result was a gun with rise and fall times of $\lesssim$ 0.1 nsec providing a 100 ma radial beam, relatively free from ringing.[13] Air dielectric coaxial cable with a rise time of $<$ 0.1 nsec was used to deliver the drive pulses from the generator to the gun.

However, due to the transit time of the electron beam traversing the 6.35 mm to the inside surface of the 12.7 mm diameter electron collector, the effective electron pulse was triangular in shape and approximately 2.2 nsec long. Figure 4 is a photograph of the modified 7587 Nuvistor electron gun.

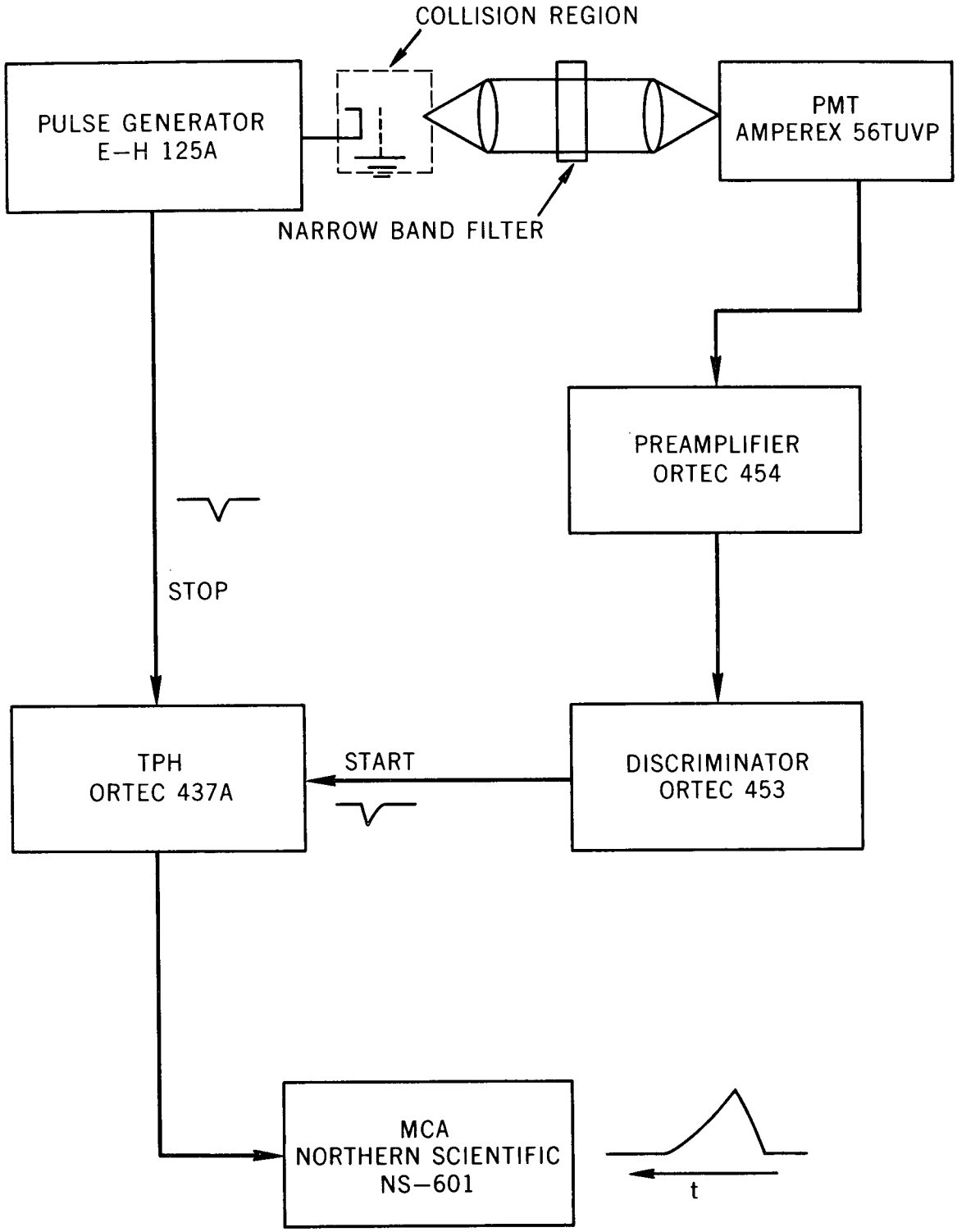

Figure 3. Block diagram of the apparatus.

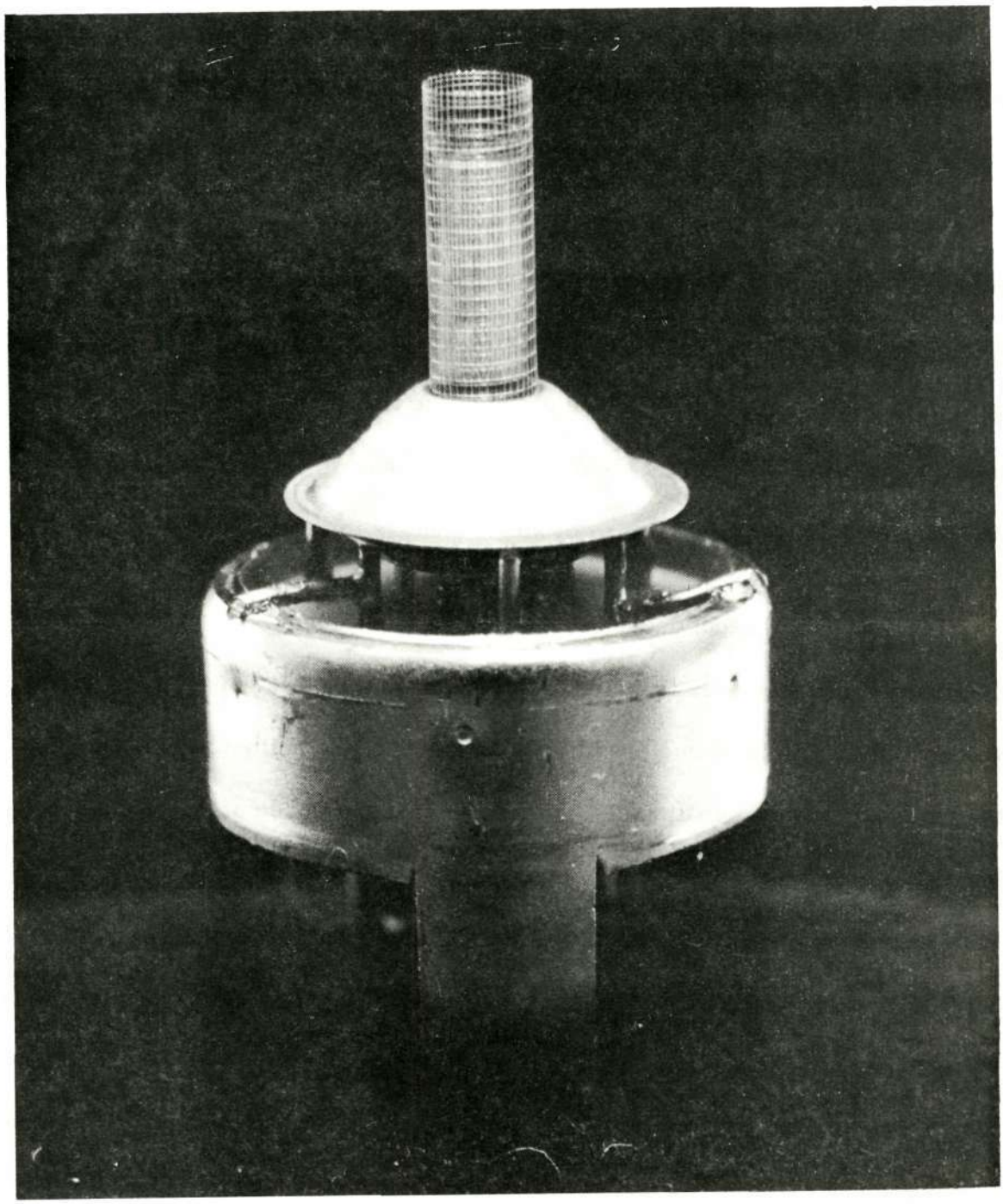

Figure 4. Modified Nuvistor electron gun. The diameter of the grid structure is approximately 1.5 mm. Note additional ground connections from the grid support to the case to improve characteristics of the electrode structure.

Transit Time and Impurity Problems

The data were adversely affected by two very difficult problems. Although the ~2 ns rise time of the photomultiplier could be picked off to an accuracy ~0.1 nsec, (and the overall timing capability of the entire apparatus was ~0.2 nsec), the lifetime curves showed a rounding of the peak after the electron pulse was known to be turned off. This rounding was found to be due to a time uncertainty or time spread in the transit time of the electron pulse through the multiplier section of the PMT. The shape of the transit time spread was determined as follows, and may be the only measurement of electron transit time spread associated with fast timing of single photons in existence.

The fast (~1.04 nsec) decay 3900 Å spectral component of P-15 phosphor was measured[14] and then used to evaluate the transit time spread of the PMT. Data were obtained with the same conditions pertaining to the helium runs except that the light source was a coating of P-15 phosphor on the inside of the electron collector. Computer analysis of the data resulted in a decay curve distorted by the PMT transit time spread. This decay curve was simulated on an analog computer, Fig. 5, by convoluting a truncated adjustable-width Gaussian curve with a rectangular-pulse-excited RC integrator circuit response (i.e., the capacitor voltage as a function of time). The latter simulated the electron beam excitation of the phosphor. The results shown in Fig. 6 indicate that the PMT transit time spread was ~2.5 nsec full width @ 1/e.

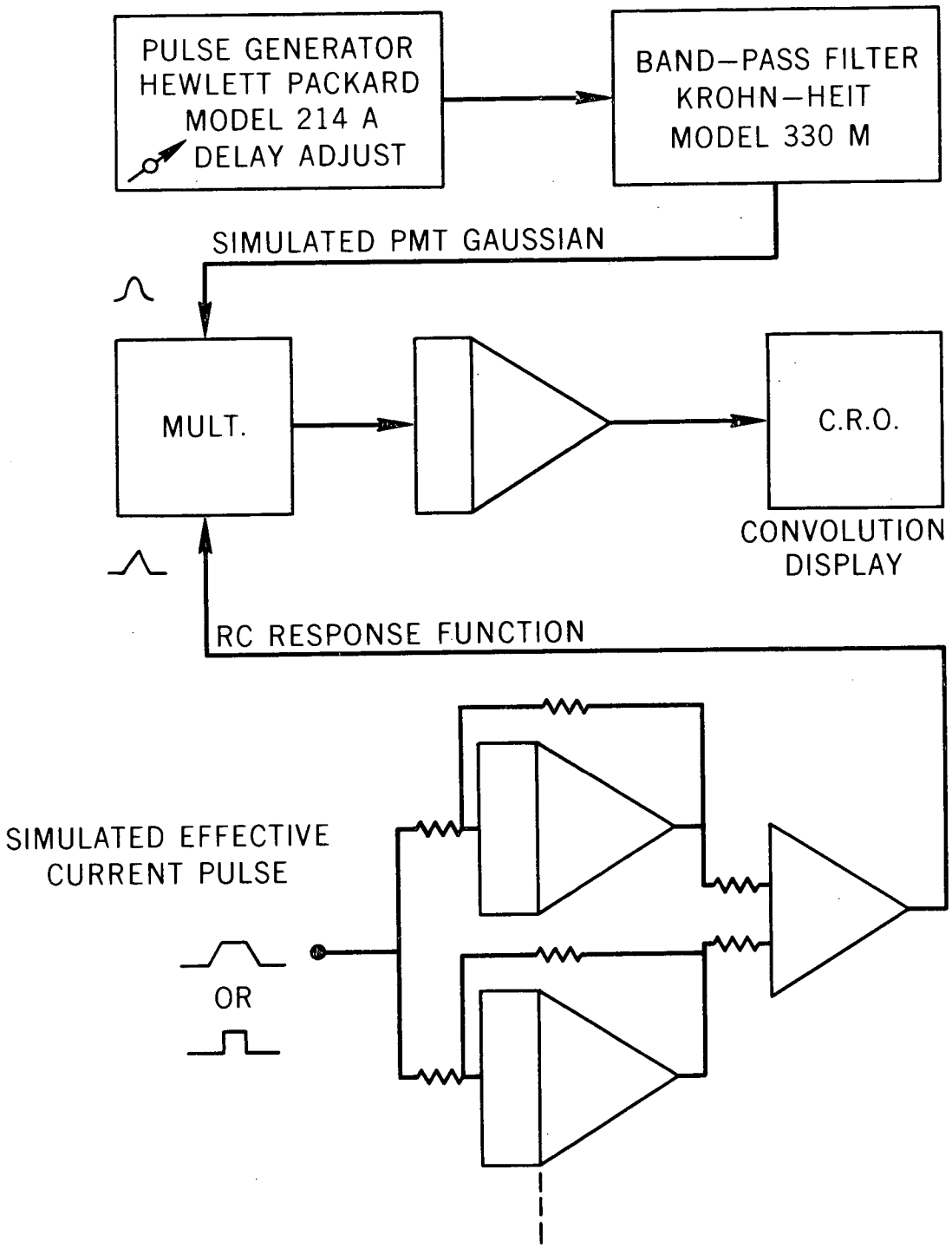

Figure 5. Analog computer for convolution calculations. The mult. unit takes the product of the PMT Gaussian function with the RC response and this is displayed on a cathode ray oscilloscope (C.R.O).

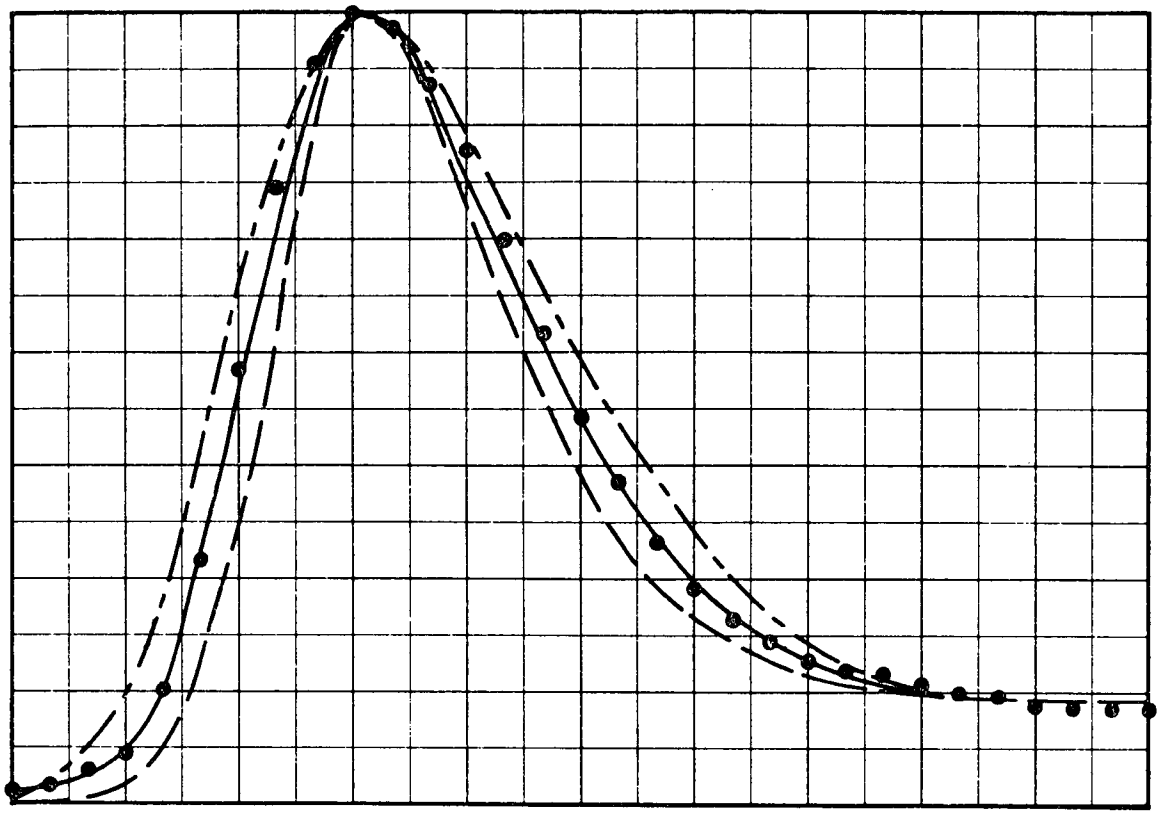

Figure 6. Analog convolutions of triangular pulse with variable-width Gaussian, with indicated best fit to 2.5 nsec. Gaussian. _ _ _ _ Gaussian Width = 3.0 nsec. ——— Gaussian Width = 2.5 nsec. — — — Gaussian Width = 2.0 nsec. ● Data.

It was found that data could be accumulated with no helium in the vacuum chamber. The resulting decay curve was composed of 2.3 nsec and 9 nsec components and is believed to be caused by CO which is known to be evolved by oxide coated cathodes. This necessitated making a high vacuum run with the MCA in the "subtract" mode after completion of each helium run in order to remove the effect of the CO background.

Data and Computer Analysis

As mentioned above, the data were rounded near the peak of excitation. This necessitated using both analog and digital computer analyses to determine the relative amounts of the four components known to be in the decay curve. It may be shown that once past the rounding of the peak, the Gaussian response of the photomultiplier will properly follow the fast components in pure exponential decays.[15] Thus, beyond the rounded part, our results were taken as composed of a sum of four known exponentials, plus an effective long lived component possibly due to some small leakage of light through the dielectric filters. A digital computer program was used to fit to this portion of the curve. An analog computer was then used to determine the cross sections necessary to produce the results obtained in the digital analysis starting at data point #54.

The analog computer analysis proceeded as follows. A time-scaled (1 nsec → 1 sec) triangular shaped pulse with 1 nsec rise- and fall-times and 0.2 nsec flat top, which simulated the experimental effective current pulse, was used to

excite computer-simulated RC integrator circuits. The RC integrator circuits simulated the He^+ excited state level populations, where the level populations n_j follow the differential equation:

$$\dot{n}_j(t) + A_j n_j(t) = \frac{I(t)}{e} \rho \ell' Q_{oj} \equiv Q_{oj} S_o s(t) \qquad (1)$$

and the charge on the capacitor of an ideal integrator obeys the differential equation:

$$\dot{q}_j(t) + (RC)_j^{-1} q_j(t) = E_j(t)/R = E_{oj} e(t)/R$$

The analogy is complete if one identifies:

$n_j = q_j$, $A_j = (RC)_j^{-1}$, and $Q_{oj} S_o = E_{oj}/R$, $s(t) = e(t)$ where:

n_j is the population of atomic level j,

A_j is the Einstein coefficient for level j,

$A_j = \sum_k A_{jk} = \tau_j^{-1}$, τ_j is the lifetime of level j,

Q_{oj} is the apparent level cross section,

S_o is the magnitude of the input current pulse,

$I(t)$ is the beam current, so that I/e = no. of e^-/sec. in the beam

ℓ' is the effective beam length,

E_{oj} is the magnitude of the jth capacitor voltage, and

ρ is the gas density.

The capacitor voltages were convoluted with a simultaneously-generated time-scaled 2.5 nsec Gaussian which simulated the effect of the PMT transit time spread. Each of the integrator voltages convoluted separately with the

Gaussian resulted in an analog computer output voltage which was set proportional to the digital computer amplitude for each decay component at point #54. (The shape of the curve generated when all of the RC simulations were convoluted simultaneously with the Gaussian showed good agreement with the shape of the original data curve, thereby confirming the validity of the technique.) Adjusting the analog computer amplitude to match the original digital computer amplitude at point #54 yielded a cross section correction factor for each decay component.

Other corrections included an adjustment factor of

$$\left[\frac{1-e^{-A_j \Delta t}}{A_j \Delta t}\right]$$

to compensate for the effects of the finite channel width Δt (1/3 nsec) of the MCA.

Because the final data resulted from a helium run followed by a reverse run which removed the effects of the background, the random fluctuations in the data which were analyzed arose from two normal distributions. These errors add as the square root of the sum of the squares of the individual fluctuations. Taking this into account, it was found that 54% of the data points were within $\pm 1\sigma$ of the calculated values, 95% were within $\pm 2\sigma$, and 98.8% were within $\pm 3\sigma$, as compared to 68%, 95%, and 99.7%, respectively, for perfect normal distributions.

The data are somewhat biased due to some ringing in the electron gun circuit. In order to verify that the final computer analysis represented the best

possible fit to the data, the relative amounts of the three fastest components were varied. As shown in Fig. 7, the quoted results represent a minimum in the chi-square distributions. The final computed curve is compared to the data in Figure 8, where the first 54 points of the data is an analog fit and the remaining portion is the digital computer fit.

Other errors which could affect the final results include uncertainties in the analog convolution due to uncertainty in the value of the PMT transit time spread and uncertainties caused by nonrandom noise and impurities. Estimates of these contributions and estimates of the final total errors are given in Table II.

Comparison with Previous Study

Our results agree only qualitatively with the one other time-resolved study of the 4686 Å radiation reported by Anderson and Hughes (AH).[16] We find a long lived component of $\tau = 44 \pm 0.5$ nsec. in the decay scheme which agrees well with the finding of a 46 nsec. component by AH. They have attributed this component to the excitation of some long lived process. It may be that the long lived component is due to the leakage of neutral helium deexcitation radiation through our dielectric optical filters, or, in the case of AH's results, due to scattered light leakage through their monochromator. The total line cross section for 4686 Å radiation has been measured to be approximately 10^{-20} cm^2. The total cross section for all singlet levels in atomic helium is on the order of 10^{-17} cm^2, at 200 eV. Spectrometers typically have 0.1% scattered light transmission, and

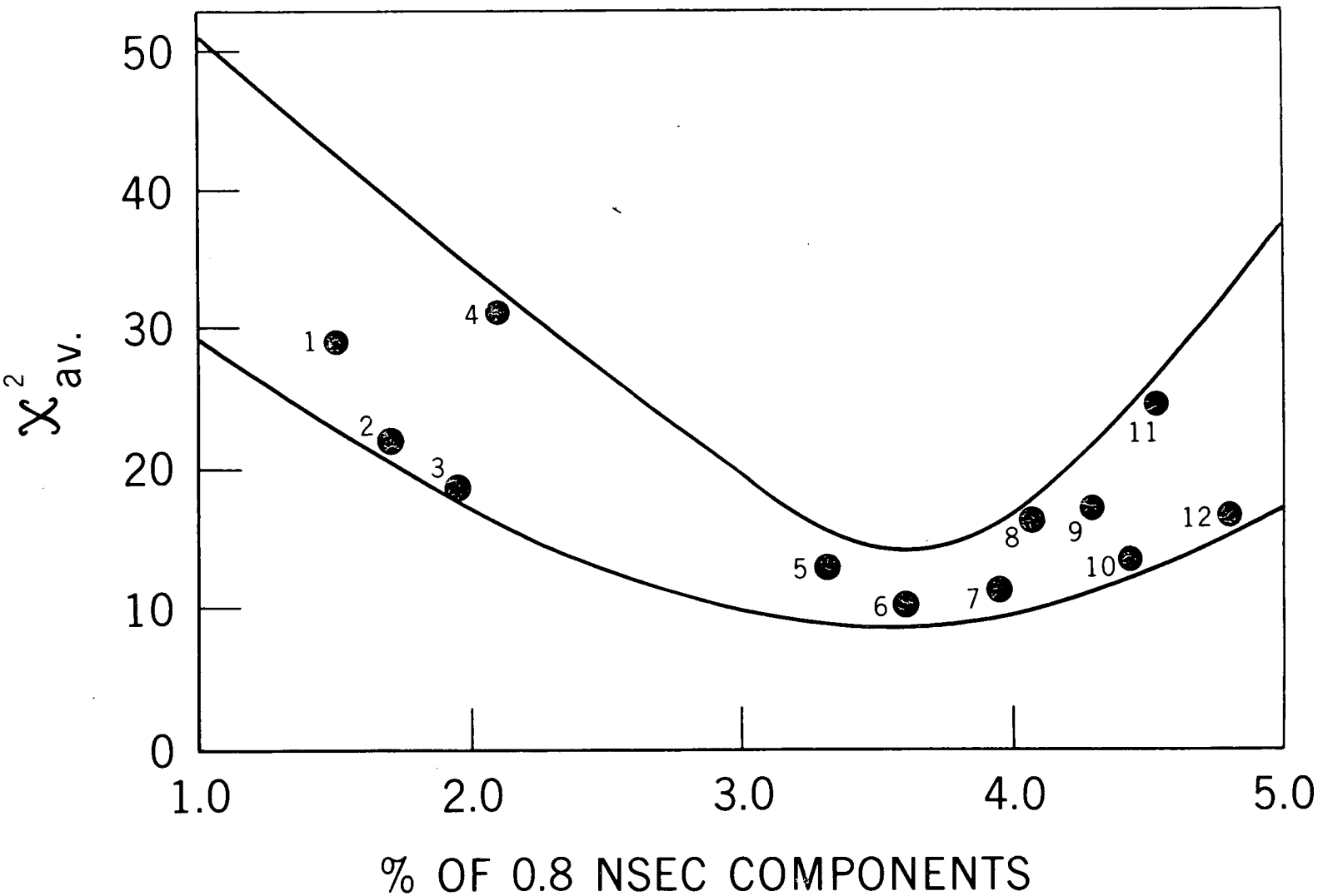

Figure 7. Variation of X^2 average with relative magnitude of Q(4P). The Relative Percentages of Q(4D) and Q(4F) respectively are: Point #1: 13.1, 43.7, #2: 11.9, 44.2, #3: 10.4, 44.8, #4: 18.8, 38.5, #5: 4.1, 41, #7: 11.5, 42, #8: 10.2, 43.9, #9: 10.1, 42.5, #10: 11.5, 43, #11: 8.7, 44.5, #12: 10.1, 43.5. Chi-square values greater than one are due to the fact that the data come from the difference between two random distributions.

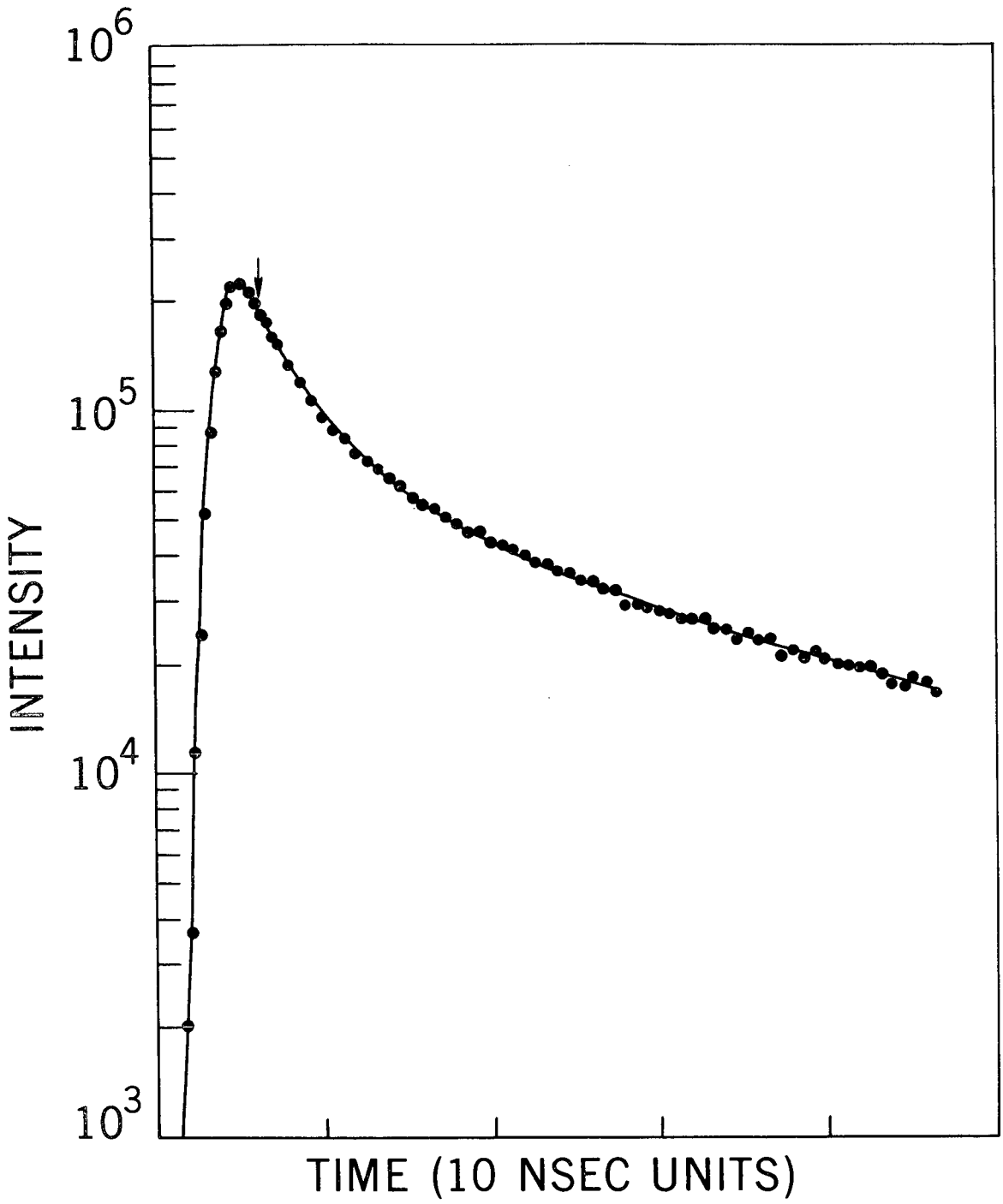

Figure 8. Comparison of the data with the computed curve. Arrow indicates location of juncture of analog fit to computer fit. Only alternate data points have been plotted.

Table II

Error Analysis

Component	Analog Convolution	Digital Computer Analysis	Non-Random Noise and Impurities	Total
4^2P - 0.78 nsec	± 10%	+15% -50%	± 40%	+65% -90%
4^2D - 2.20 nsec	± 5%	+10% -24%	± 30%	+40% -54%
4^2F - 4.50 nsec	± 2%	±10%	± 20%	±25%
4^2S - 14.50 nsec	0	± 5%	5%	±10%

dielectric filters also suffer from similar leakage. Hence, the vast majority of light in the excitation region which emanates from excited atomic helium levels may be responsible for the observed long lived component.

Further, it would not seem that the long lived component may be attributed to cascade. The lifetimes of the higher lying He^+ states which might cascade appreciably into the He^+ n = 4 level are considerably shorter than 44 nsec. Assuming that the cross sections to a given angular momentum level decrease as the cube of the principal quantum number, we have estimated that our results are affected by less than 2% by cascade. Our use of a very short electron excitation pulse strongly discriminated against the excitation of the long lived, higher He^+ levels.

We find a considerably larger fraction of the decay complex coming from the fast decay components than do AH. Disregarding the 44 nsec component, they find percentages of the remaining light flux from the combined fast components and a 10 - 14 nsec. component to be 52% and 48% respectively. Using our cross section ratios we calculate, assuming a 20 nsec. pulse as typical of the shorter pulses employed by AH, percentages of combined fast components and a 14 nsec. component of 80% and 20% respectively. Although this discrepancy is difficult to explain, it is not outside experimental error.

Conclusions

The derived relative cross sections are presented in Table III. It is apparent that the dipole channel is populated appreciably more than the other channels. This result seems intuitively reasonable, but it is not in good agreement with the Born calculations.[9, 10, 11] In the first Born calculations which have been carried out, the ground state helium level has been taken as the product of two screened hydrogenic wave functions, the final He level of hydrogenic wave function with $Z' = 2$, and the ionized electron approximated by the continuum wave function in a coulomb field of screened charge Z''.[10, 11] The choice of Z'' for the continuum wave function has been somewhat arbitrary, often chosen simply to insure orthogonality between initial and final states.[11] Lee and Lin investigated the effects of changing Z'' from 1.69 to 1.45 in the calculation of Q (He^+, 4S) and found only a 25% variation in the predicted cross section. However, the amplitude for simultaneous ionization and excitation to $\ell \neq 0$ levels has a different form from that for the $\ell = 0$ levels, and the resulting cross sections to $\ell \neq 0$ levels are very dependent upon the overlap between the continuum wave function of the ionized electron and the wave function of one of the helium ground state 1S electrons. This overlap, in turn, is extremely sensitive to the choice of Z''. Dalgarno and McDowell point out that changing Z'' from 1.69 to 1.45 changed their Q (He^+, 4P) cross section more or less continuously from zero to 2.8×10^{-21} cm^2. Lee and Lin find that a change in Z'' from 1.45 to 1.53 makes a factor of two change in their Q (He^+, 4F) cross section.

Table III

Results, Compared with Theory[11]

Ratio	Experiment	Theory
$\frac{Q\ (He^+\ 4^2P)}{Q\ (He^+\ 4^2S)}$	$16.00\ ^{+10.0}_{-14.0}$	0.36
$\frac{Q\ (He^+\ 4^2D)}{Q\ (He^+\ 4^2S)}$	$1.10\ ^{+00.4}_{-00.6}$	0.084
$\frac{Q\ (He^+\ 4^2F)}{Q\ (He^+\ 4^2S)}$	0.74 ± 00.2	0.001

Nevertheless, it is difficult to rationalize the large discrepancy between our experimental results and the theoretical predictions, particularly the much larger than expected P state cross section. It may well be that other channels of excitation must be considered in order to explain the results.

It should be noted that we did not find any appreciable variation in the shape of the decay curves with respect to changes in pressure or beam current which indicates that neither recombination nor excitation of ground state He^+ created by previous electronic excitations were appreciable.

REFERENCES

(1) R. H. Hughes and L. D. Weaver, Phys. Rev. 132, 710 (1963); also J. Chem. Phys. 47, 346, (1967).

(2) R. M. St. John and C. C. Lin, J. Chem. Phys. 41, 195, (1964), also J. Chem. Phys. 47, 347, (1967).

(3) H. P. Larson and R. W. Stanley, J. Opt. Soc. Am. 57, 1439, (1967).

(4) H. R. Moustafa Moussa and F. J. DeHeer Physica 36, 646, (1967).

(5) W. R. Bennett Jr., G. N. Mercer, P. J. Kindlmann, B. Wexler, and H. Hyman, Phys. Rev. Letters 17, 987, (1966).

(16) R. J. Anderson and R. H. Hughes, Phys. Rev. A5, 1194, (March 1972).

(17) J. A. Jordan, Jr., et. al., JOSA 57, 530, (April 1967).

FIGURE CAPTIONS

Figure 1. Total cross section, QHe^+ (4 → 3) vs. impact electron energy (Hughes and Weaver).

Figure 2. Partial Grotrian diagram for He^+, showing the possible modes of decay in the n = 4 → n = 3 complex.

Figure 3. Block diagram of the apparatus.

Figure 4. Modified Nuvistor electron gun. The diameter of the grid structure is approximately 1.5 mm. Note additional ground connections from the grid support to the case to improve characteristics of the electrode structure.

Figure 5. Analog computer for convolution calculations. The mult. unit takes the product of the PMT Gaussian function with the RC response and this is displayed on a cathode ray oscilloscope (C.R.O).

Figure 6. Analog convolutions of triangular pulse with variable-width Gaussian, with indicated best fit to 2.5 nsec. Gaussian. _ _ _ _ _ Gaussian Width = 3.0 nsec. ——— Gaussian Width = 2.5 nsec. _ _ _ _ Gaussian Width = 2.0 nsec. • Data.

Figure 7. Variation of X^2 average with relative magnitude of Q(4P). The Relative Percentages of Q(4D) and Q(4F) respectively are: Point #1: 13.1, 43.7, #2: 11.9, 44.2, #3: 10.4, 44.8, #4: 18.8, 38.5, #5: 4.1, 41, #6: 12.9, 41, #7: 11.5, 42, #8: 10.2, 43.9, #9: 10.1, 42.5, #10: 11.5, 43, #11: 8.7, 44.5, #12: 10.1, 43.5. Chi-square values greater than one are due to the fact that the data come from the difference between two random distributions.

Figure 8. Comparison of the data with the computed curve. Arrow indicates location of juncture of analog fit to computer fit. Only alternate data points have been plotted.